SciMedCentral

Journal of Pharmacology & Clinical Toxicology

Research Article

Stereoselective Analysis of Tartaric Acid Using Complexation with Eu^{3+}-Tetracycline and Capillary Electrophoresis

Douglas B Craig[1,2]*, Joshua W Hollett[2], Sumaiya Abas[2], and Brynne K Riehl[3]

[1,2]Department of Chemistry, University of Winnipeg, Canada
[3]Department of Biology, University of Winnipeg, Canada

***Corresponding author**
Douglas B Craig, Department of Chemistry, University of Winnipeg, Winnipeg, Manitoba, Canada

Submitted: 04 September 2023
Accepted: 03 October 2023
Published: 06 October 2023
ISSN: 2333-7079

Keywords
- Capillary electrophoresis
- Europium tetracycline
- luminescence
- Molecular modelling
- Tartaric acid

Abstract

Tartaric acid was incubated with Eu^{3+}-tetracycline and the sample was analyzed by capillary electrophoresis utilizing post-column laser-induced luminescence detection. The D-isomer was detected at concentrations as low as 5 µM. The L-isomer was not detected. The juice from fresh loquat fruit was found to contain 41 mM D-tartaric acid. Further study was undertaken to determine the basis for the stereoselectivity. Molecular modelling was not consistent with the D-isomer forming a more stable complex. The rates of dissociation of the Eu^{3+}-tetracycline-tartarate complexes during the separation were determined. Rates were consistent with the complex with the L-isomer degrading during the separation.

INTRODUCTION

Tartaric acid (2,3-dihydroxybutanedioic acid, CAS number 526-83-0) is a by-product of fermentation. It is used in baking (cream of tartar), as a non-toxic household cleaner, and industrially it is used along with its derivatives in the pharmaceutical industry. It is a dicarboxylic acid with pK_a values of 3.0 and 4.3. Tartaric acid contains 2 chiral centers and exits in 3 sterioisoforms; L-(+)-tartaric acid (2R,3R), D-(-)-tartaric acid (2S,3S), and the meso-form, DL-tartaric acid (2R,3S). L-tartaric acid is common in nature and is sometimes referred to as 'natural' tartaric acid. The D-form is rare in nature [1], and its presence in appreciable concentrations is largely limited to the metabolism of some microorganisms. The DL-form does not occur in nature [2-4].

Tartaric acid has been measured spectrophotometrically upon treatment with $FeSO_4$, H_2O_2 and NaOH [5]. It has also been analyzed using complexation with vanadate and flow injection spectrophotometry, providing a detection limit of 500 µM [6]. Gravimetric analysis through precipitation as calcium tartrate [7], or lead tartrate [8], potentiometry [9,10], capillary electrophoresis [11], and liquid chromatography [12,13], have been used for the non-stereoselective analysis of tartaric acid.

Determination of the D- and L-isomers of tartaric acid has been achieved after separation by capillary electrophoresis in the presence of a chiral selector and detection at 250 nm (Lumex Instruments, https://www.lumexinstruments.com/files/DETERMINATION_OF_ORGANIC_ACIDS_ISOFORMS.pdf). Both isomers could be detected at concentrations as low as 300 µM with a 7 min separation time. A method for the measurement of L-tartaric acid based on the secondary activity of D-malate dehydrogenase and absorbance detection [2], has provided a detection limit of 20 µM. Recently, a fluorescent probe has been described that displays different colors in the presence of D- and L-tartaric acid [14].

Eu^{3+} is luminescent and its strongest emission is associated with a $^7F_{0\text{-}6} \leftarrow {}^5D_0$ transition, providing a red color [15]. This luminescence is modified by chelation with ligands which include tetracycline [16]. Eu^{3+}-tetracycline luminescence can be further modulated by replacement of water ligands with additional ligands. This has been used as a means of detection of many different analytes of biological interest including coenzyme A [17], NADPH [18], ATP and other mononucleotides [19], glycolysis and Kreb's cycle intermediates [16], phosphate [20], H_2O_2 [21,22], serum albumin [23], heparin [24], and lecithin [25]. Measurement of the formation of some of these analytes has also been used as the basis of enzyme assays [19]. In these studies, separations of mixtures of analytes were not performed. Some analytes, present in the same sample, could be distinguished by measuring luminescence half-lives [26].

Here, a report on the analysis of D-, L-, and DL-tartaric acid

using complexation with Eu^{3+}-tetracycline and separation by capillary electrophoresis utilizing post-column laser-induced luminescence detection within a sheath flow cuvette is given. This is followed by an investigation into the basis for which the different stereoisomers produce different amounts of signal.

MATERIALS AND METHODS

Reagents

All reagents were obtained from Sigma (St. Louis MO). Fresh loquat fruit imported from Japan was obtained from a local business (https://www.facebook.com/99-fresh-garden-103372768221689/).

Capillary electrophoresis (CE) instrument

Separations were performed using an in-laboratory constructed CE instrument which utilizes post-column laser-induced luminescence detection within a sheath flow cuvette. Details of the instrument, including a schematic, has been published previously [27]. The injection end of an uncoated silica capillary which was 25 cm long, with inner and outer diameters of 10 and 145 µm respectively, as well as a 0.5 mm diameter platinum wire connected to a high voltage power supply, was placed into a buffer containing vessel in the injection carousel. Approximately 1 mm of external polyamide coating was removed by flame from the detection end of the capillary before its insertion into a quartz sheath flow cuvette containing a 250 by 250 µm inner bore (Hellma, Markham ON). The capillary was grounded through the sheath flow buffer within the cuvette. The 10 mW output at 407 nm of a solid state laser (Coherent, Santa Clara CA) was focused using a 6.3 X, N.A. 0.2 microscope objective (Melles Griot, Carlsbad CA) approximately 10 µm below the detection end of the capillary. Emission was collected at 90° using a 60X, N.A. 0.7 microscope objective (Universe Kogaku, Oyster Bay NY) then passed through a 615DF45 optical filter (Omega Optical, Brattleboro VT) and a slit, and onto a photomultiplier tube (PMT, Hamamatsu model 1477, Shizuoka Japan). The analog signal was collected at 25 Hz and digitized using a Pentium 4 computer through a PCI-MIO-16XE I/O board utilizing LabView™ software (National Instruments, Austin TX). The same board was used to control the electrophoresis voltage and set the PMT bias to 1100 V. The buffer flowing through the sheath flow cuvette was 25 mM HEPES containing 50 mM TRIS base (pH unadjusted, ~8.0). The running buffer was 15 mM HEPES with 30 mM TRIS base and contained 40% (v/v) formamide (pH unadjusted). Since formamide hydrolyses slowly, fresh running buffer was made daily by adding formamide to 25 mM HEPES containing 50 mM TRIS base (pH unadjusted, ~8.0). Samples were electrokinetically injected into the capillary for 5 s at an electrical field of 200 Vcm^{-1} and separated at an electrical field of 800 Vcm^{-1} (injection end positive). Data was analyzed using IgorPro™ (WaveMetrics, Lake Oswego OR) and peak heights were determined using PeakFit™ (Systat Software, San Jose CA).

Sample preparation

Samples contained buffer, either 50 or 200 µM Eu^{3+}-tetracyline, and tartaric acid of varying concentrations. All samples were incubated at room temperature for at least 30 min prior to injection to allow the complex to form. When the sample contained organic solvent, a volume of the buffer was replaced by the solvent.

RESULTS AND DISCUSSION

100 µM solutions of D-, L- and DL-tartaric acid were made in 25 mM HEPES containing 50 mM TRIS base (pH unadjusted, ~8.0) and 200 µM Eu^{3+}-tetracycline. Samples were separated by capillary electrophoresis using 15 mM HEPES containing 30 mM TRIS base and 40% (v/v) formamide (pH unadjusted) as the running buffer. The resultant electropherograms are depicted in Figure 1. The blank contained no tartaric acid. In the blank, a peak with a migration time of 58 s was observed which is due to the luminescent Eu^{3+}-tetracycline complex. The presence of 40% formamide in the running buffer decreased peak trailing substantially and increased the electroosmotic flow, thus shortening the run time. A second peak with a migration time of 66 s was observed in the presence of both D and DL-tartaric acid but not in the presence of L-tartaric acid. Furthermore, the peak was larger in the presence of D-tartaric acid. Separations were run for 150 s. After each separation, the capillary was flushed for 60 s with 100 mM NaOH containing 10 mM EDTA followed by 90 s with running buffer. Total time per sample analysis was therefore 5 min.

D-tartaric acid analysis

The methodology used was selective for the D-form of tartaric acid over that of the L-isomer. The DL-form of this compound was not a subject of inquiry in this study since it is not known to exist in nature.

To assess the ability to detect D-tartaric acid, separations were performed on solutions of 25 mM HEPES containing 50 mM TRIS base (pH unadjusted, ~8.0) and 50 µM Eu^{3+}-tetracycline as well as D-tartaric acid ranging in concentrations from 200 µM to 5 µM (Figure 2). The relationship between signal and concentration, shown in the lower graph of Figure 3, has a curvature to it. This deviation from linearity was likely due to depletion of the Eu^{3+}-tetracycline as the concentration of D-tartaric acid was increased. When the samples contained 200 µM Eu^{3+}-tetracycline the curvature was reduced (Figure 3, upper graph). The background signal was largely caused by the trailing Eu^{3+}-tetracycline peak and thus was increased when the Eu^{3+}-tetracycline was present at the higher concentration. This higher background prevented the detection of a clear peak for the sample containing 5 µM D-tartatic acid. When the samples contained the L-isomer instead of the D-, the electropherograms were identical to that of the blank at all concentrations of both the tartaric acid and Eu^{3+}-tetracycline (data not shown).

Loquats (*Eriobotrya japonica*) are broad bushy trees that have been grown in Japan for the past 1000 years (University of California, Agriculture and Natural Resources, http://fruitsandnuts.ucdavis.edu/dsadditions/Loquat_Fact_Sheet/).

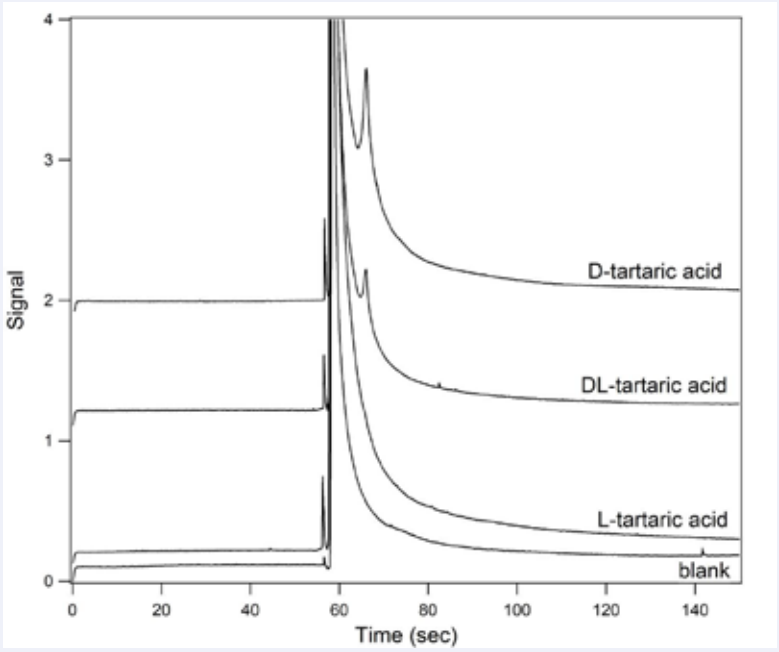

Figure 1 Electropherograms of the separations of complexes of D-, L- and DL-tartaric acid with europium tetracycline. 100 μM solutions of D-, L- and DL-tartaric acid were made in 25 mM HEPES containing 50 mM TRIS base (pH unadjusted, ~8.0) and 200 μM Eu^{3+}-tetracycline. Samples were separated by capillary electrophoresis and the resultant electropherograms are shown. The lowest trace is that of a blank and contained no tartaric acid. The peak eluting at 58 s is due to the Eu^{3+}-tetracycline complex. The trace second to the bottom is that of the sample containing L-tartaric acid. It is indistinguishable from the blank. The second from the top trace is that from the sample containing DL-tartaric acid. A peak is observed at 66 s that is due to the Eu^{3+}-tetracycline-tartaric acid complex. The top trace is from the sample containing D-tartaric acid. The 66 s peak is enlarged in this sample.

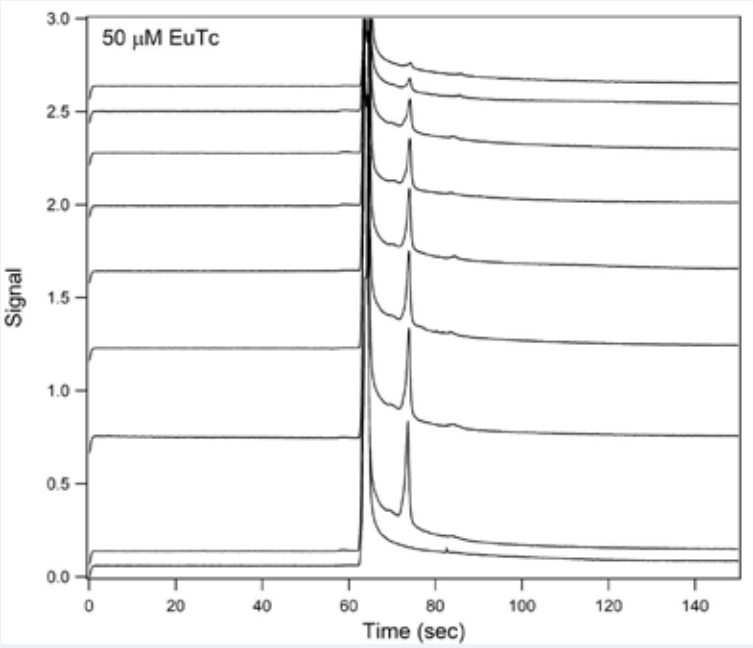

Figure 2 Separations of complexes of europium tetracycline with differing concentrations of D-tartaric acid. The resultant electropherograms are shown for separations performed on solutions of 25 mM HEPES containing 50 mM TRIS base (pH unadjusted, ~8.0) and 50 μM Eu^{3+}-tetracycline and D-tartaric acid ranging in concentrations from 200 μM to 5 μM. The bottom trace is that of a blank. The traces above it are for samples containing 200, 150, 100, 75, 50, 25, 10 and 5 μM D-tartaric acid.

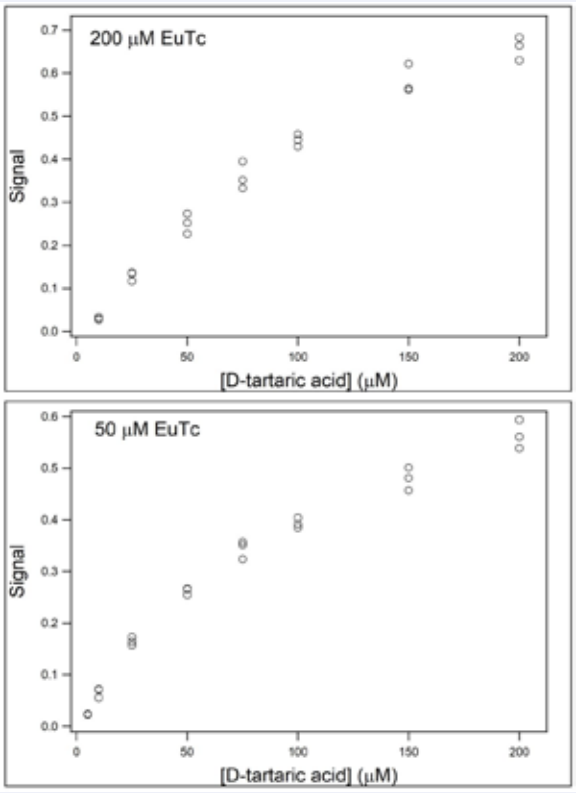

Figure 3 Relationship between signal and concentration of D-tartaric acid. The relationship between peak height and [D-tartaric acid] is shown for two different concentrations of Eu^{3+}-tetracycline. In the presence of 50 µM Eu^{3+}-tetracycline a peak is observed when the [D-tartaric acid] is 5 µM (lower graph). However the relationship between peak height and concentration starts to curve above 25 µM. In the presence of 200 µM Eu^{3+}-tetracycline the relationship is linear up to 100 µM and deviates somewhat at higher concentrations. However, no peak is detected at 5 µM.

The oval fruit is 3-5 cm long and has an orange skin and flesh. The Metabolomics Innovation Center (https://www.metabolomicscentre.ca/) identifies that D-tartaric acid has been detected, but not quantified, in loquat fruit. Furthermore, they suggest that D-tartaric acid could potentially be used as a biomarker for foods that contain loquat since it rarely occurs elsewhere naturally.

(https://foodb.ca/compounds/FDB001110).

Figure 4 depicts the resultant electropherogram from the analysis of the juice obtained from a fresh loquat fruit. In the lower trace, the juice was diluted 200-fold into sample buffer containing 200 µM Eu^{3+}-tetracycline. In the middle trace, the sample was spiked with 100 µM D-tartaric acid and in the upper trace the sample was spiked with both 100 µM D-tartaric acid and 2.5 µM citric acid. An increased height of the peaks at 66 and 77 s was observed upon spiking with D-tartaric acid and citric acid respectively. This is consistent with the peaks at 66 and 77 seconds being D-tartatic acid and citric acid respectively. A method to detect citric acid by formation of a complex with Eu^{3+}-tetracycline and separation using capillary electrophoresis was previously reported [28]. The concentrations of D-tartaric acid and citric acid in undiluted loquat juice were calculated to be 41 mM and 55 µM respectively.

Selectivity for D- over L-tartaric acid

The remainder of this study aimed to understand the basis for the selectivity of the D-isomer over that of the L-isomer. There are two possible explanations for why no peak was observed for the L-isomer; either no complex formed between Eu^{3+}-tetracycline and the L-isomer of tartaric acid or the complex formed but dissociated during the separation.

The luminescence signals of solutions of D-, L- and DL-tartaric acid made in 25 mM HEPES containing 50 mM TRIS base (pH unadjusted, ~8.0) and 200 µM Eu^{3+}-tetracycline were measured using a Cary Eclipse benchtop fluorimeter. No separation was used. Excitation was at 407 nm (5 nm slip width) and emission was collected at 615 nm (5 nm slit width). When the tartaric acid concentration was increased from zero to 200 µM, there was an increase in signal of approximately 50%. The increase in signal for all three stereoisoforms of tartaric acid were nearly identical (Figure 5). This suggests that all three were indistinguishable with respect to their ability to form complexes with Eu^{3+}-tetracycline. This result was inconsistent with that depicted in Figure 1. This suggested that the differences in signal obtained for the different isomers was associated with the separation.

In a previous study the capillary electrophoresis separation of

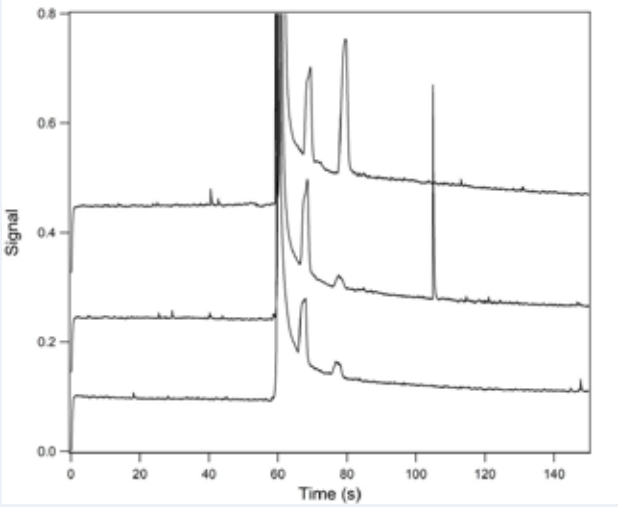

Figure 4 Analysis of the juice from loquat fruit. Resultant electropherogram from the analysis of loquat juice. In the lower trace the juice was diluted 200-fold into sample buffer containing 200 µM Eu^{3+}-tetracycline. In the middle trace the sample was spiked with 100 µM D-tartaric acid and in the upper trace the sample was spiked with both 100 µM D-tartaric acid and 2.5 µM citric acid.

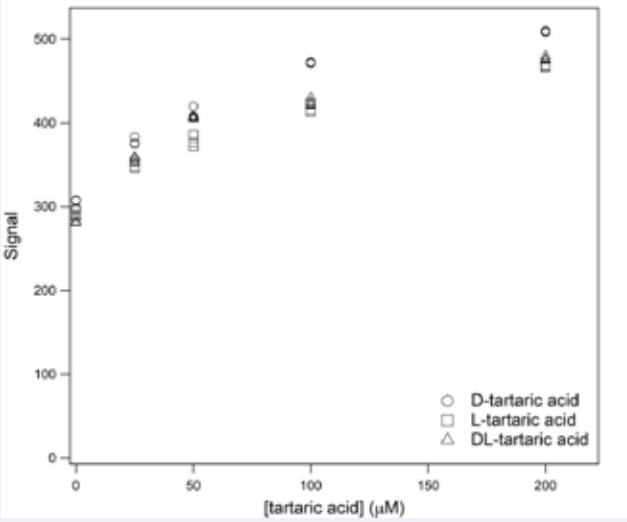

Figure 5 Signal for complexes between tartaric acid and europium tetracycline in the absence of a separation. The luminescence signals of solutions of D-, L- and DL-tartaric acid made in 25 mM HEPES containing 50 mM TRIS base (pH unadjusted, ~8.0) and 200 µM Eu^{3+}-tetracycline are shown. No separation was used. Excitation was at 407 nm and emission was collected at 615 nm.

complexes of several different metabolites with Eu^{3+}-tetracycline was reported. No peaks were detected for several metabolites that were detected in the absence of a separation by other groups. It was suggested that the complexes might have dissociated during the separation [29].

$$Eu^{3+}\text{-Tc} + n(\text{tartaric acid}) \rightleftharpoons Eu^{3+}\text{-Tc-(tartaric acid)}_n$$

In the sample Eu^{3+}-tetracycline, tartaric acid and the Eu^{3+}-tetracycline-tartaric acid complexes were present together in equilibrium. However as the separation proceeded the complex was separated from the free Eu^{3+}-tetracycline and free tartaric acid in the capillary. Thus, the complex was no longer in equilibrium with its components and might have been expected to start to dissociate. One possible explanation for the selectivity for the D-isomer is that it forms a more stable complex. This possibility was assessed using molecular modeling.

Molecular modeling

The structure and energetics of possible Eu^{3+}-tetracycline complexes with one, two and three tartarates (both L and

D-isomers) were explored using density functional methods within the ORCA computational chemistry package [30]. Molecular geometries were optimized using the B3LYP density functional approximation [31-33], the def2-TZVP basis set [34], with ZORA relativistic correction and the SARC/J auxiliary basis set [35-40]. Geometries were optimized in solvent (SMD water solvation) and vibrational frequencies were calculated and analyzed to ensure potential energy surface minima had no imaginary frequencies. The effect of water solvation was simulated using the SMD solvation model [40]. Using many different user-generated guesses guided by chemical intuition (e.g., H-bonding, oxygen atom donors), multiple structures corresponding to minima on the potential energy surface were identified for one, two and three tartarate ligands. For the one-tartarate and three-tartarate complexes (where all ligands were the same isomer), there was no substantial free energy difference (< 7 kJ mol^{-1}) found between the lowest energy complex involving D-tartarate or L-tartarate.

Four of the two-tartarate complexes are shown in Figure 6. The two structures on the left [(1) and (3)] involve D-tartarate, while the two on the right [(2) and (4)] involve L-tartarate. The bottom right structure, (4), has the lowest relative free energy of all the two-tartarate structures observed, while the bottom left structure, (3), has the lowest relative free energy of the complexes involving D-tartarate. At room temperature, and given the expected accuracy of the computational model, a free energy difference of 5.1 kJ mol^{-1} is insignificant and therefore provides no explanation of the experimental observations. However, another D-tartarate complex was observed that has significant interaction between the tartarates and both the Eu^{3+} ion and tetracycline [complex (1)]. The same interaction could not be achieved with two L-tartarates due to the opposing chirality [complex (2)]. The D-tartarate complex has a relative free energy that is lower than the L-tartarate structure by 22.2 kJ mol^{-1} which is attributable to the reduction of hydrogen bonding in the L-tartarate structure.

Complexes (3) and (4) have lower relative free energies, however the balance of their interactions may play a role in their relative kinetic stability in solution. The D-tartarates of complex (3) do not interact with each other and leave room for other tartarates or solvent molecules to interact with Eu^{3+}. The L-tartarates of complex (4) do not directly interact with the tetracycline. Energy calculations of the Eu^{3+}-(L/D-tartarate)$_2$

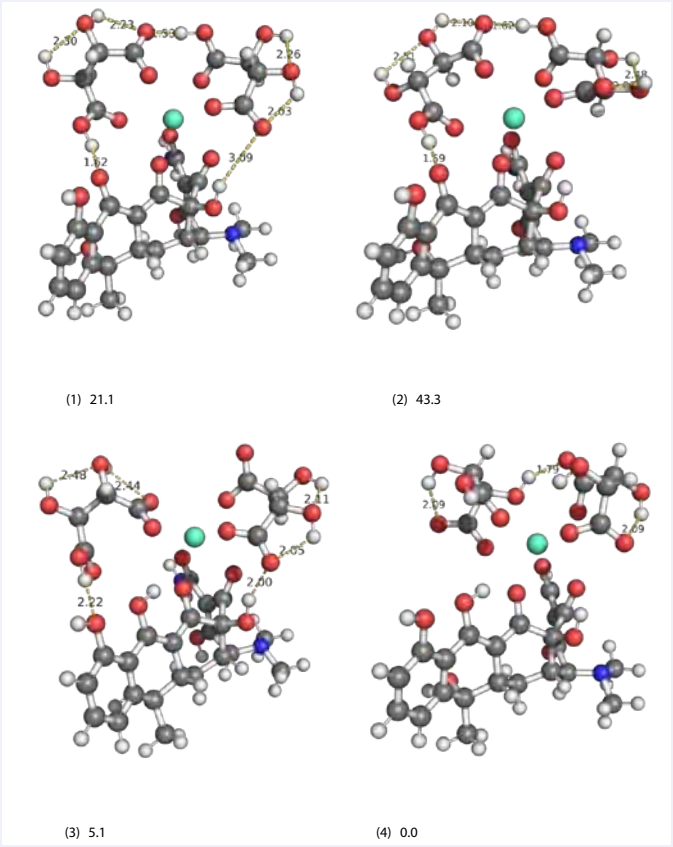

Figure 6 Molecular modelling derived structures of the europium-tetracycline complexes with tartaric acid. Structures of Eu^{3+}-tetracycline-(tartarate)2 complexes determined with density functional theory and the SMD solvent model are shown. D-tararate structures are in the left column (1) and (3), and L-tartarate structures are on the right. (2) and (4). Hydrogen bonds are indicated with yellow dashes and distance given in Angstrom. Calculated relative free energies (kJmol-1) are shown adjacent to each structure label.

fragment of complexes (1)-(4) reveals that the Eu^{3+}- tartarate interactions are responsible for the low free energy of complex (4), and the interactions between the D-tartarates, Eu^{3+}, and tetracycline are much more balanced in complex (1). The D-isomer is able to form a complex with two hydrogen bonds to the tetracycline, seven oxygens interacting with Eu^{3+}, and a perimeter of intra and intermolecular hydrogen bonds. For the similar structure involving L-tartarate, (2), the chirality forces the carboxylate group to choose between interacting with Eu^{3+} or forming a hydrogen bond with tetracycline. The ability of only one enantiomer to form such a complex with the chiral Eu^{3+}-tetracycline complex due to geometric constraints is a reasonable explanation for the relative stability of the complexes witnessed during the separations.

Addition of organic solvent to the sample buffer

The addition of miscible organic solvent to the sample was tested for its effect on peak heights obtained with the D-, L- and DL-isomers of tartaric acid. In this experiment, varying amounts of different miscible solvents were added to the sample buffer where the complex between the Eu^{3+}-tetracycline and the tartaric acid was formed. The running buffer used in the separation remained as previously: 15 mM HEPES containing 30 mM TRIS base and 40% (v/v) formamide (pH unadjusted, ~8.0). The effect of the presence of 0, 20, 40 and 60% (v/v) formamide, dimethylsulfoxide, N,N-dimethylformamide, acetonitrile, methanol and acetone in the sample buffer was determined for all 3 forms of tartaric acid. Tartaric acid concentration was held constant at 100 µM and the concentration of Eu^{3+}-tetracycline was maintained at 200 µM.

The addition of formamide to the sample buffer dramatically increased the signal obtained for D-tartaric acid. In the presence of 60% (v/v) formamide the signal increased approximately 10-fold. The presence of DMSO and DMF had minimal effect. A decrease in signal was observed in the presence of each of acetonitrile, methanol and acetone. No peak was observed for D-tartaric acid in both 60% (v/v) acetone and 60% (v/v) acetonitrile (Figure 7).

When an organic additive was not present in the sample buffer no peak was observed for L-tartaric acid. However the presence of formamide, DMSO or DMF resulted in the presence of a peak. Formamide had the largest effect as at 60% (v/v) a peak that was larger than that for D-tartaric acid in the absence of any organic additive was observed. No peak was observed in the presence of acetonitrile, methanol or acetone.

The effect of additives to the signal obtained for the DL-form of tartaric acid was similar to that of the D-form. The signal was increased substantially by the presence of formamide. DMSO resulted in a moderate increase in signal and DMF had minimal effect. The presence of acetonitrile, methanol and acetone resulted in a decrease in signal with no peak detected in the presence of 60% acetone.

Although the presence of formamide increased the signal obtained for D-tartaric acid, this occurred at the expense of losing selectivity for the D-form over that of the L-form. This loss of selectivity also occurred in the presence of DMSO and DMF. Selectivity was maintained in the presence of acetonitrile, methanol and acetone but the signal was decreased by the presence of these additives.

Activation Energy of Dissociation

Molecular modelling did not suggest that the complex between Eu^{3+}-tetracycline and D-tartaric acid was more stable than that for the L-isomer. One possible explanation as to why the less stable structure was detected after the CE separation while the more stable was not, is that the rate of dissociation of the L-isomer may be faster than that of the D-form. If so, the L-isomers complex could have fully dissociated during the separation while there was insufficient time for the D-isomer to do so as well. It was not possible to determine the activation energy of dissociation of the L-isomer during the separation in the absence of formamide because no peak was detected. Therefore, the activation energy was determined in the presence of formamide in the sample buffer. The activation energies of dissociation of the complex made with the D- and DL-isomers was also determined when the sample contained formamide.

Sample containing 100 µM tartaric acid, 200 µM Eu^{3+}-tetracycline, 15 mM HEPES, 30 mM TRIS base and 40% (v/v) formamide was injected into the capillary and separated at 800 Vcm^{-1} for 45 s. This was followed by a period of no separation. After this period the separation was continued. During the initial 45 s separation, the zone of Eu^{3+}-tetracycline-tartaric acid complex was separated from that of the Eu^{3+}-tetracycline. During the following period of no mobilization, the complex had extra time to dissociate. The separation was then completed and the peak height determined in order to assess how much of the complex remained relative to runs where there was no pause. This was performed for all 3 isomers of tartaric acid using several different pause times and when the central portion of the capillary was maintained at 21.5°C as well as at 4°C. Rate constants were determined using 1st order kinetic plots for each isomer at each temperature. From the determined rate constants the activation energies of dissociation of the complexes formed with each of the 3 isomers of tartaric acid were calculated.

Figure 8 shows the resultant electropherograms for separations of the complex using L-tartaric acid performed at 21.5°C without a pause in the separation and with pauses of 10, 20 and 40 s (lower graph). As the pause period increased, the peak representing the Eu^{3+}-tetracycline-tartaric acid complex decreased and a new peak, eluting at 68 s, increased. As the complex dissociated during the pause, Eu^{3+}-tetracycline accumulated at the position in the capillary where the complex was sitting, which was partway along the length of the capillary. Upon resumption of the separation, this Eu^{3+}-tetracycline produced the peak that appeared between that of the residual complex and the peak for the Eu^{3+}-tetracycline that did not initially form the complex.

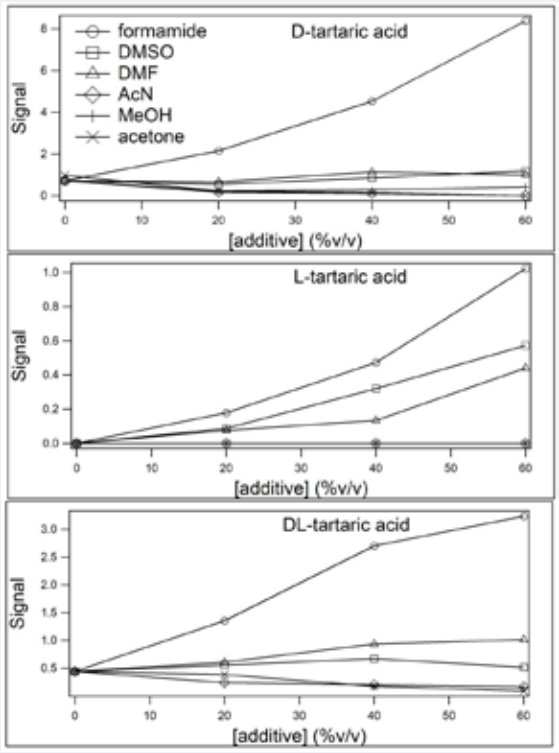

Figure 7 Effect of added organic solvent on signal obtained from europium tetraclcine-tartaric acid complexes. The effect of different organic solvents, present from zero to 60% (v/v), on the peak heights observed for D- (top trace), L- (middle trace) and DL-tartaric acid (bottom trace) are shown. Tartaric acid concentration was held constant at 100 μM and the concentration of $Eu3^{+}$-tetracycline was maintained at 200 μM.

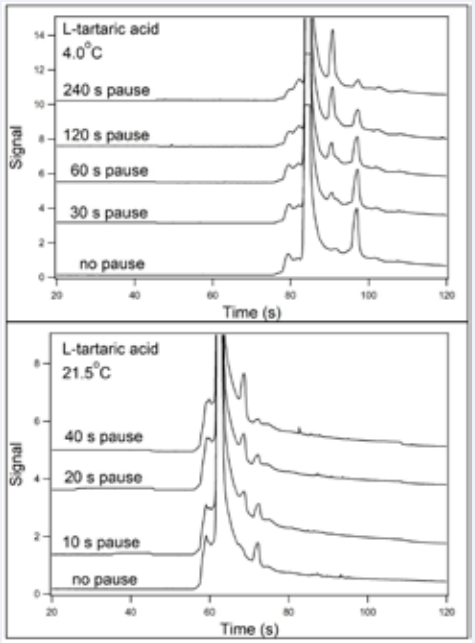

Figure 8 Experimental determination of the rate constants for the dissociation of the europium tetracycline-tartaric acid complexes. The resultant electropherograms for separations of the complex using L-tartaric acid performed at 21.5°C without a pause in the separation and with pauses of 10, 20 and 40 s (lower graph) is shown. The upper trace shows the electropherograms for the separations performed at 4°C without a pause and with pause periods of 30, 60, 120 and 240 s.

The upper graph shows the separation of the complex with L-tartaric acid at 4.0°C. Retention times of all peaks were increased due to the slower electroosmotic flow at the lower temperature. Longer pause periods were required for dissociation of the complex. Similar separations at both 21.5 and 4.0°C were performed using the complexes formed with D- and DL-tartaric acid (data not shown).

First order rate constants were determined graphically using plots of ln(peak height from paused separation/peak height from un-paused separation) versus time of the pause for all 3 isomers and at both temperatures. The rate constants at 21.5 and 4.0°C were used to determine the activation energy of dissociation of the complexes with the three different isomers of tartaric acid (Figure 9). Activation energies of dissociation were calculated to be 91, 77 and 69 $kJmol^{-1}$ for the complexes made using the D-, DL- and L-isomers of tartaric acid respectively. This suggests that the reason why the D-isomer produced a peak in the separation when the sample contained no formamide was due to its higher activation energy and therefore lower rate of dissocation. The separation time was too short for the complex to fully dissociate. The L-isomer yielded no peak due to its higher rate of dissociation causing no complex to remain by the time the separation was completed. The DL-isoform yielded an intermediate size peak due to it having an intermediate rate of dissociation.

CONCLUSION

Eu^{3+}-tetracycline is luminescent and its luminescence is modulated by complexation with many different analyte molecules. In this study, complexes were made with tartaric acid and the samples separated using capillary electrophoresis. L-tartaric acid is common in nature and the D-isomer is very uncommon. The DL-isomer does not exist in nature. This protocol was used to develop a stereoselective means for tartaric acid analysis. Samples were separated on a 25 cm long capillary at 800 Vcm^{-1}. Separations were run for 150 s each with the analyte eluting after 66 s. The capillary was flushed between runs yielding a total analysis time of 5 min per sample. No peak was detected for the L-isomer whereas the D-isomer produced a peak. D-tartaric acid was detected at 5 μM. This system was used to determine that the concentration of D-tartaric acid in loquat fruit was 41 mM. Loquat is one of the few natural sources of D-tartaric acid and this compound has been suggested to be a potential marker for the presence of loquat in foods.

The second part of this study aimed to understand the basis for the stereoselective nature of this analysis. Solutions containing Eu^{3+}-tetracycline and D-, L- and DL-tartaric acid were analyzed on a benchtop fluorimeter in the absence of any separation. All three isomers behaved indistinguishably, indicating that all three equally formed a complex with Eu^{3+}-tetracycline. This suggested that the cause of the observed difference in this study was not due to the ability to form a complex, but rather was a by-product of the separation itself. Molecular modelling was performed to determine if the D-isomer formed a more thermodynamically stable complex with Eu^{3+}-tetracycline. The modelling suggested that the D-isomer could form a complex that cannot be attained by the L-isomer. However, the complex determined to be the most stable was obtained with the L-isomer. The modelling therefore

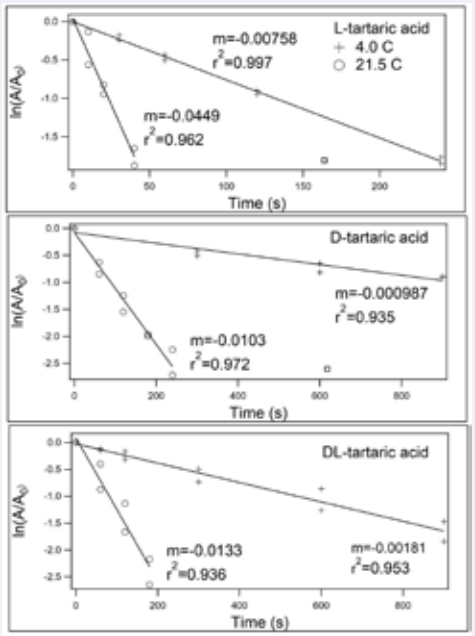

Figure 9 Aarhenius plots for the dissociation of the europium tetracycline-tartaric acid complexes. The relationship between ln(peak height from paused separation/peak height from un-paused separation) versus length of time of the pause for L- (top graph), D- (middle graph), and DL-isomers (bottom graph) are shown for separations performed at 21.5 and 4.0°C.

did not provide a clear answer as to why a complex was observed post-separation with the D-isomer but not for the L-isomer. One possibility is that the activation energy of dissociation was lower for the L-isomer leading to a more rapid breakdown of the complex. However, in order to measure the rate of breakdown of the complexes, it was necessary to modify the system through the addition of formamide to allow for the detection of the complex with the L-isomer. The rates of dissociation of the complexes with the D-, L- and DL-isomers during the separations at 21.5 and 4°C were used to calculate the activation energies of dissociation. The complex with the L-isomer showed the lowest activation energy of dissociation, the D-isomer the highest, and the DL-isomer an intermediate value. This is consistent with the L-isomer yielding no peak in the separation due to it dissociating before the separation was completed, the L-form producing the largest peak since did not completely dissociate, and the DL-isomer producing an intermediate size peak due to a rate of dissociation between that of the two other isomers.

ACKNOWLEDGEMENTS

This project was supported by grants from the Natural Sciences and Engineering Research Council (Canada).

REFERENCES

1. Ukaji Y, Soeta T. Acetogenin (Polypriopionate) Derived Auxiliaries: Tartaric Acid. Comprehensive Chirality. 2012; 2: 176-201.
2. Tsukatani T, Matsumoto K. Enzymatic quantification of L-tartrate in wines and grapes by using the secondary activity of D-malate dehydrogenase. Biosci Biotechnol Biochem. 1999; 63: 1730-1735.
3. Yew WS, Fedorov AA, Fedorov EV, Wood BM, Almo SC, Gerlt JA. Evolution of enzymatic activities in the enolase superfamily: D-tartrate dehydratase from Bradyrhizobium japonicum. Biochemistry. 2006; 45: 14598-14608.
4. Kim OB, Lux S, Unden G. Anaerobic growth of Escherichia coli on D-tartrate depends on the fumarate carrier DcuB and fumarase, rather than the L-tartrate carrier TtdT and L-tartrate dehydratase. Arch Microbiol. 2007; 188: 583-589.
5. Anderson AK, Rouse AH, Letonoff TV. A colorimetric method for the determination of tartaric acid. Ind Eng Chem Anal. Ed. 1933; 5: 19-20.
6. Rangel AOSS, Tóth IV. Sequential determination of titratable acidity and tartaric acid in Wines by flow injection spectrophotometry. Analyst. 1998; 123: 661-664.
7. Luque de Castro MD, González-Rodríguez J, Pérez-Juan P. Analytical Methods in Wineries: Is It Time to Change? Food Reviews Int. 2005; 21: 231-265.
8. Manley CH. The determination of tartaric acid as lead tartrate. Analyst. 1937; 62: 526-530.
9. Sales MGF, Amaral CEL, Delerue-Matos CM. Determination of tartaric acid in wines by FIA with tubular tartrate-selective electrodes. Fresenius J Anal Chem. 2001; 369: 446-450.
10. Akhond M, Tashkourian J, Hemmateenejad B. Simultaneous determination of ascrobic, citric, and tartaric acids by potentiometric titration with PLS calibration. J Analytical Chemistry. 2016; 61: 804-808.
11. Castineira A, Pena RM, Herrero C, Garcia-Martin S. Analysis of Organic Acids in Wine by Capillary Electrophoresis with Direct UV Detection. J Food Composition Analysis. 2002; 15: 319-331.
12. Prenesti E, Toso S, Daniele PG, Zelano V, Ginepro M. Acid-base chemistry of red wine: analytical multi-technique characterisation and equilibrium-based chemical modelling. Analytica Chimica Acta. 2004; 507: 263-273.
13. Ivanova-Petropulos V, Petruševa D, Mitrev S. Rapid and Simple Method for Determination of Target Organic Acids in Wine Using HPLC-DAD Analysis. Food Analytical Methods. 2020; 13: 1078-1087.
14. Hu M, Yuan YX, Wang W, Li DM, Zhang HC, Wu BX, et al. Chiral recognition and enantiomer excess determination based on emission wavelength change of AIEgen rotor. Nat Commun. 2020; 11: 1-10.
15. Shriver D, Weller M, Overton T, Rourke J, Armstrong F. Inorganic Chemistry, 2014, 6th Edition, New York: WH Freeman and Company.
16. Lin Z, Wu M, Schaeferling M, Wolfbeis OS. Fluorescent imaging of citrate and other intermediates in the citric acid cycle. Angew Chemie. 2004; 43: 1735-1738.
17. Peng Q, Ge X, Jiang C. A new spectrofluorometric probe for the determination of trace amounts of CoA in injection, human serum and pig livers. Anal Sci. 2007; 23: 557-561.
18. Peng Q, Hou F, Ge X, Jiang C, Gong S. Fluorimetric study of the interaction between nicotinamide adenine dinucleotide phosphate and tetracycline-europium complex and its application. Anal Chim Acta. 2005; 549: 26-31.
19. Schaferling M, Wolfbeis OS. Europium tetracycline as a luminescent probe for nucleoside phosphates and its application to the determination of kinase activity. Chemistry. 2007; 15: 4342-4349.
20. Lischynski JR, Goltz DM, Craig DB. Measurement of phosphate in small samples using capillary electrophoresis with laser-induced luminescence detection. J Liq Chromatogr. R.T. 2019; 41: 1-6.
21. DaSilva FR, Courrol LC, Tarelho LVG, Gomes L, Vieira ND. Enhancement of europium luminescence in tetracycline-europium complexes in the presence of urea hydrogen peroxide. J Fluoresc. 2005; 15: 667-671.
22. Durkop A, Wolfbeis OS. Nonenzymatic direct assay of hydrogen peroxide at neutral pH using the Eu_3Tc fluorescent probe. J Fluoresc. 2005; 15: 755-761.
23. Jiang CQ, Luo L. Spectrofluorometric determination of human serum albumin using a tetracycline-europium complex. Anal Lett. 2004; 37: 1129-1137.
24. Zhu XJ, Wang XL, Jiang CQ. Spectrofluorometric determination of heparin using a tetracycline-europium probe. Anal Biochem. 2005; 341: 299-307.
25. Wang T, Jiang CQ. Spectrofluorimetric determination of lecithin using a tetracycline-europium probe. Anal Chim Acta. 2006; 561: 204-209.
26. Lin Z, Wu M, Wolfbeis OS. Time-resolved fluorescent chirality sensing and imaging of malate in aqueous solution. Chirality. 2005; 17: 464-469.
27. Chen DY, Adelhelm K, Cheng XL, Dovichi NJ. A simple laser-induced fluorescence detector for sulforhodamine 101 in a capillary electrophoresis system: Detection limits of 10 yoctomoles or six molecules. Analyst. 1994; 119: 349-352.
28. Craig DB, Lischynski JR, Cardoso ICC. Citrate analysis using capillary electrophoresis and complexation with Eu^{3+}-tetracycline. BioMetals. 2018; 31: 1043-1049.
29. Craig DB, Hiebert Z. Analysis of complexes of metabolites with europium tetracycline using capillary electrophoresis coupled with laser induced luminescence detection. BioMetals. 2017; 30: 449-459.
30. Neese F, Wennmohs F, Becker U, Riplinger C. The ORCA quantum chemistry program package. J Chemical Physics. 2020; 152: 224108.

31. Vosko SH, Wilk L, Nusair M. Accurate spin-dependent electron liquid correlation energies for local spin density calculations: a critical analysis. Can J Phys. 1980; 58: 1200-1211.

32. Lee C, Yang W, Parr RG. Development of the Colle-Salvetti correlation-energy formula into a functional of the electron density. Phys Rev B. 1988; 37: 785-789.

33. Becke AD. Density-functional thermochemistry. III. The role of exact exchange. J Chem Phys. 1993; 98: 5648-5652.

34. Weigend F, Ahlrichs R. Balanced Basis Sets of Split Valence, Triple Zeta Valence and Quadruple Zeta Valence Quality for H to Rn: Design and Assessment of Accuracy. Phys Chem Chem Phys. 2005; 7: 3297-3305.

35. Pantazis DA, Neese F. All-Electron Scalar Relativistic Basis Sets for the Lanthanides. J Chem Theory Comput. 2009; 5: 2229-2238.

36. Weigend F. Accurate Coulomb-Fitting Basis Sets for H to Rn. Phys Chem Chem Phys. 2006; 8: 1057-1065.

37. Pantazis DA, Chen XY, Landis CR, Neese F. All-Electron Scalar Relativistic Basis Sets for Third-Row Transition Metal Atoms. J Chem Theory Comput. 2008; 4: 908-919.

38. Pantazis DA, Neese F. All-Electron Scalar Relativistic Basis Sets for the Actinides. J Chem Theory Comput. 2011; 7: 677-684.

39. Pantazis DA, Neese F. All-Electron Scalar Relativistic Basis sets for the 6p Elements. Theor Chem Acc. 2012; 131: 1292.

40. Marenich AV, Cramer CJ, Truhlar DG. Universal Solvation Model Based on Solute Electron Density and on a Continuum Model of the Solvent Defined by the Bulk Dielectric Constant and Atomic Surface Tensions. J Phys Chem B. 2009; 113: 6378-6396.